

# The Surface Characterization of Carbonaceous Nanoparticles and Flame Soot: the Chemical Composition of the Interface

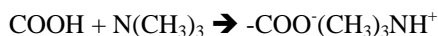
Ari Setyan<sup>1</sup>, J.-J. Sauvain<sup>1</sup>, M. Riediker<sup>1</sup>, M. Guillemin<sup>1</sup> and Michel J. Rossi<sup>\*2</sup>

<sup>1</sup>IST (Institut Universitaire Santé au Travail), rue du Bugnon 19, CH-1005 Lausanne

<sup>2</sup>LPAS/ENAC/ISTE, Station 6, EPFL, CH-1015 Lausanne

There are various ways at characterizing combustion nanoparticles from a microscopic point of view. Examples are pyrolysis and thermogravimetric measurements, extraction behavior (EC/OC), elemental analysis, surface spectroscopies as well as imaging techniques (HRTEM, HRSEM). The chemical composition of aerosol nanoparticles is of interest because it may reveal both the source as well as its physical-chemical properties to some extent. However, virtually nothing is known about the chemical composition of the interface of such nanoparticles. Information about the interface may prove useful to understand the interaction of aerosol particles with biological substrates such as cell membranes, biological fluids such as lung lining fluids and solid supports for the purpose of understanding the adhesion of nanoparticles. What we propose here is a novel method at characterizing the surface composition of collected nanoparticles using a titration method by specific gas phase probe molecules. In conjunction with a metric of the surface of these nanoparticles such as the measured BET (Brunauer-Emmett-Teller) or geometrical surface obtained from electrical mobilities we arrive at the **density** of surface functional groups located at the interface of aerosol nanoparticles. These surface functional groups were identified using their specific interaction with each of the probe gas molecules. Although we lack information on the assignment of a specific surface functional group to a given molecular species present on the nanoparticle we have the assurance that these functional groups are located at the interface, accessible to a gas phase probe molecule. From a different vantage point, the probe gases “interrogate” the interface for specific reaction sites that are therefore “visible” from the gas phase.

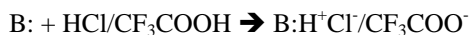
We have used six different probe gases, namely  $\text{N}(\text{CH}_3)_3$ ,  $\text{NH}_2\text{OH}$ ,  $\text{CF}_3\text{COOH}$ ,  $\text{HCl}$ ,  $\text{O}_3$  and  $\text{NO}_2$ . The governing chemical reactions are briefly described in the following. Trimethylamine ( $\text{N}(\text{CH}_3)_3$ ) heterogeneously interacts with surface acidic groups represented here by a surface carboxyl group and leads to a salt:



Surface aldehydes and ketones react with  $\text{NH}_2\text{OH}$  and yield an oxime after  $\text{H}_2\text{O}$  elimination:



Basic oxides at the interface, represented by  $\text{B:}$ , both react with the acidic probe gases  $\text{HCl}$  and  $\text{CF}_3\text{COOH}$ . Basic surface oxides on carbonaceous particles preferentially react with acetic acid compared to  $\text{HCl}$  such that the ratio of the respective reaction yields obtains an indication of the presence of basic oxides if this ratio is greater than unity. In the past, both acidic and basic oxides located on the surface of carbonaceous particles have been found that solely consist of C, O and H:



Oxidizable surface groups are expected to react with oxidants such as O<sub>3</sub> and NO<sub>2</sub>:



How do we know that it is the above reactions that are occurring during a surface titration? There are additional reactions that in principle may occur based on the published literature. However, the application of the three criteria listed below are relevant to the present reaction conditions and led us to exclusively propose the above reactions. The three **constraints** may be formulated as follows: The heterogeneous reaction must be:

- Fast, typically on the time scale of  $1/k_{\text{esc}}$  corresponding to roughly  $\sim 10$  s
- Occurring at low pressure:  $\sim 10^{-3}$  mbar and at
- Ambient temperature

We have used a Knudsen flow reactor in order to determine the number of probe gas molecules necessary to saturate the uptake of a powdered sample. The flow reactor was equipped with molecular beam-modulated phase sensitive detection using an electron-impact quadrupole mass spectrometer. The raw data consist of the number  $N_i^M$  of molecules taken up per mg of the powdered substrate. Another way to normalize the raw data was to reference the primary observable  $N_i^M$  to unity surface of the aerosol using the measured BET surface area of the sample. Still another way was to reference  $N_i^M$  to a formal monolayer expressed in per cent of a formal molecular monolayer. All three numbers are given in the Table. The listed results emphasize the **large variability** of the surface reactivity akin to the chemical surface composition in terms of the density of surface functional groups across all examined samples of carbonaceous nanoparticles which is visible proof that the chemical surface properties depend on the source of combustion as well as on aging processes in the case of collected Diesel particles. When considering the abundance of the functional group densities obtained from all six probe gases one easily sees that the amorphous carbon Printex 60 has the lowest, and FS 101 the largest functional group density. In addition, the used Knudsen reactor method also yields the reaction probabilities or uptake coefficients  $\gamma$  that express the fractional number of probe gas collisions that lead to irreversible removal of the probe gas under the chosen experimental conditions. These  $\gamma$  values have been obtained using the geometrical surface area of the sample support. A look at the Table reveals that there is no obvious correlation with the uptakes  $N_i^M$  which points towards the absence of a common reaction mechanism for these probe gas reactions. Only detailed chemical kinetic modeling necessitating additional experimental data under differing conditions may reveal the elementary reaction mechanism.

In conclusion, we have shown that

- The combustion source determines the detailed surface/interface composition in terms of the densities of functional groups
- The surface is multifunctional, e.g. acidic and basic surface sites coexist at the interface of carbonaceous particles as well as partially oxidized (carbonyl functions) and reduced ones.
- The proposed method allows a **quantitative** comparison between aerosols of different origin, e.g. from different combustion sources or different environmental origin in terms of  $N_i^M \propto \alpha \delta \gamma$ .

# The Surface Characterization of Carbonaceous Nanoparticles and Flame Soot: the chemical composition of the interface

*A. Setyan<sup>1</sup>, J.-J. Sauvain<sup>1</sup>, M. Riediker<sup>1</sup>, M. Guillemin<sup>1</sup>  
and M. J. Rossi<sup>2</sup>*

<sup>1</sup> Institut Universitaire Romand de Santé au Travail (IST), Université de Lausanne et Université de Genève, CH-1005 Lausanne, Suisse

<sup>2</sup> Laboratoire de Pollution Atmosphérique et Sol (LPAS), Station 6, Ecole Polytechnique Fédérale de Lausanne (EPFL), CH-1015 Lausanne, Suisse



ÉCOLE POLYTECHNIQUE  
FÉDÉRALE DE LAUSANNE

Generous Funding by: Secretariat for Education and Research (SER) of Switzerland (COST) and NANOTOX program, Agence Nationale de Recherche (ANR), France

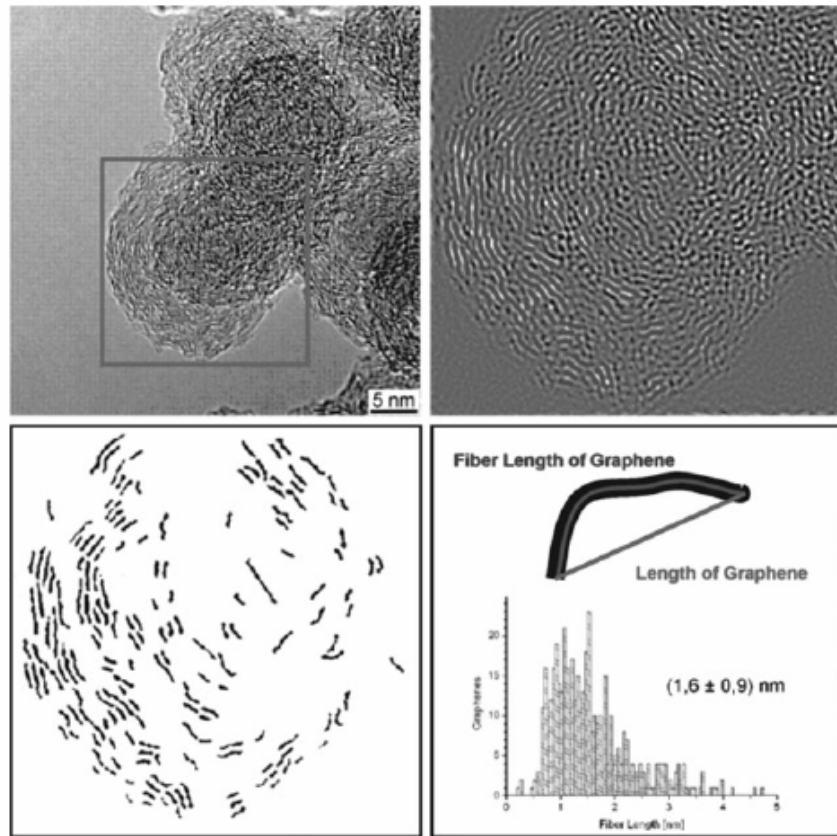


Fig. 2 Extraction of graphene sizes from HRTEM images of soot. Image selection, threshold analysis, particle selection, analysis of particles and obtained histogram.

Table 2  $sp^2/sp^3$  quantification

	$N_{sp^2}$ (%)	$N_{sp^3}$ (%)
GfG soot	54	46
Euro IV soot	66	34
BS soot	76	24
Furnace soot	77	23
Lamp black	77	23
Graphite (HOPG)	100	0

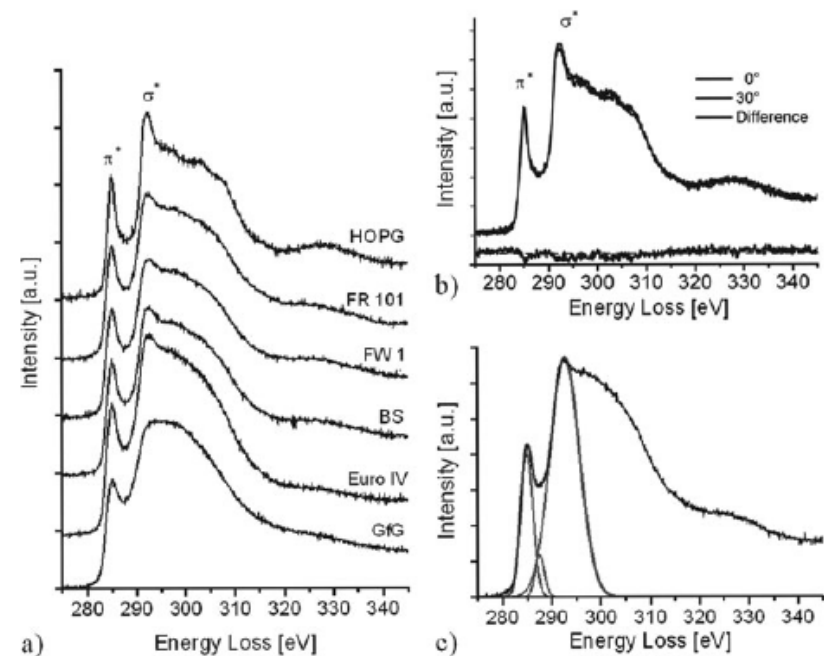
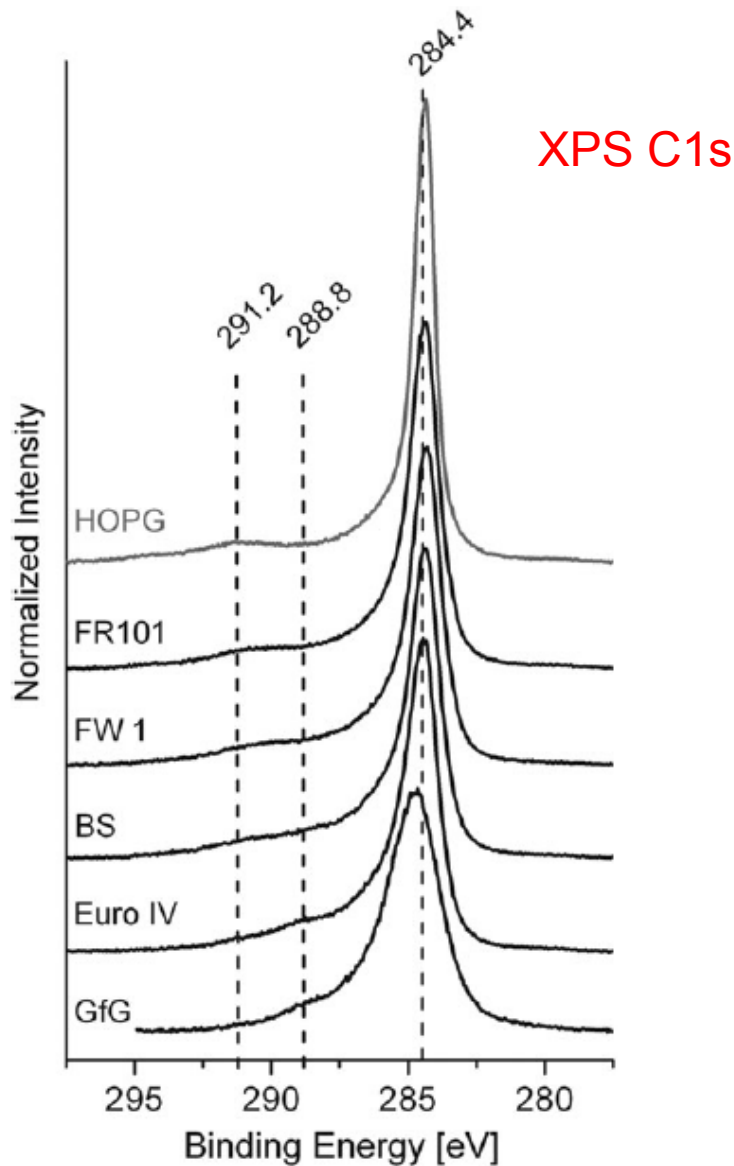
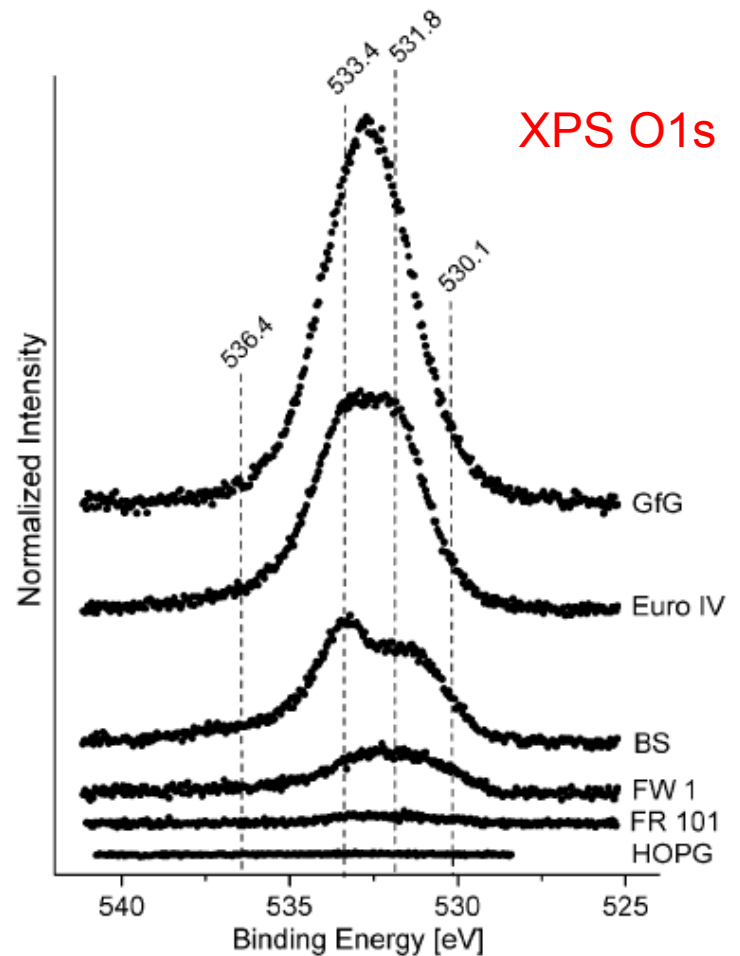


Fig. 3 Carbon-K-ionization edges of the investigated carbon materials: (a) GfG soot (GfG), diesel engine soot (Euro IV and BS), carbon black (FW 1 and FR 101) and graphite (HOPG). (b) Energy loss spectra for HOPG in different orientations. (c) Fit of spectra to deduce the  $sp^2/sp^3$  hybridization ratio.



**Fig. 4** XPS C1s spectra from the carbonaceous materials: GfG (GfG), diesel engine soot (Euro IV and BS), carbon black (FW 1 and FR 101) and graphite (HOPG). The spectra are offset for clarity.



**Fig. 6** XPS O1s spectra from the carbonaceous materials: GfG soot (GfG), diesel engine soot (Euro IV and BS), carbon black (FW 1 and FR 101) and graphite (HOPG). The spectra are offset for clarity.

## Resulting CORRELATIONS

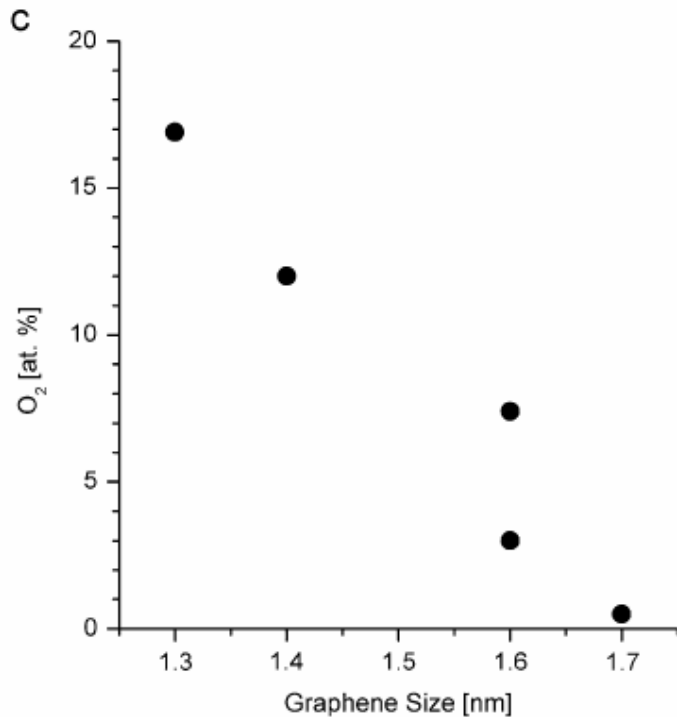
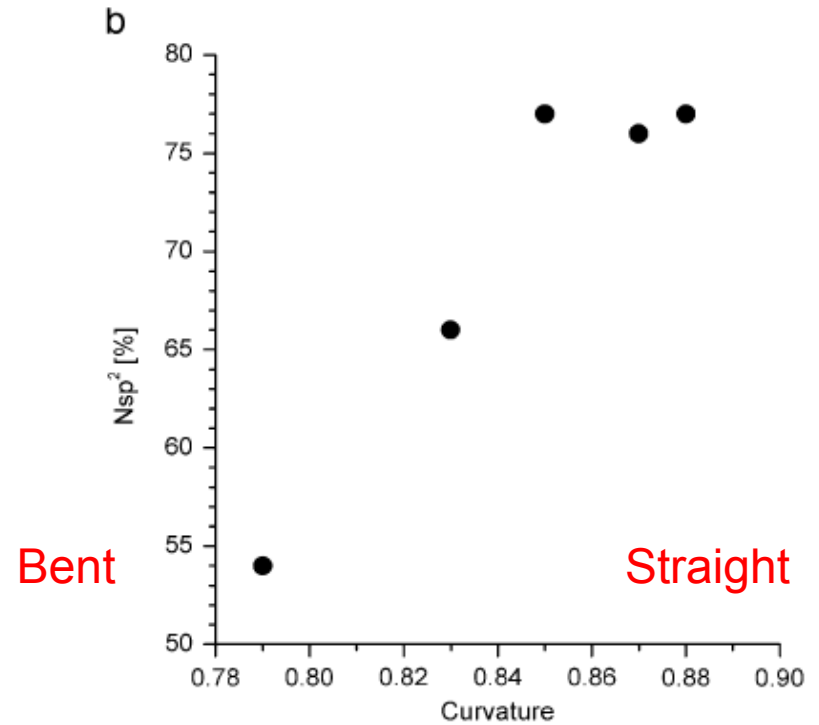
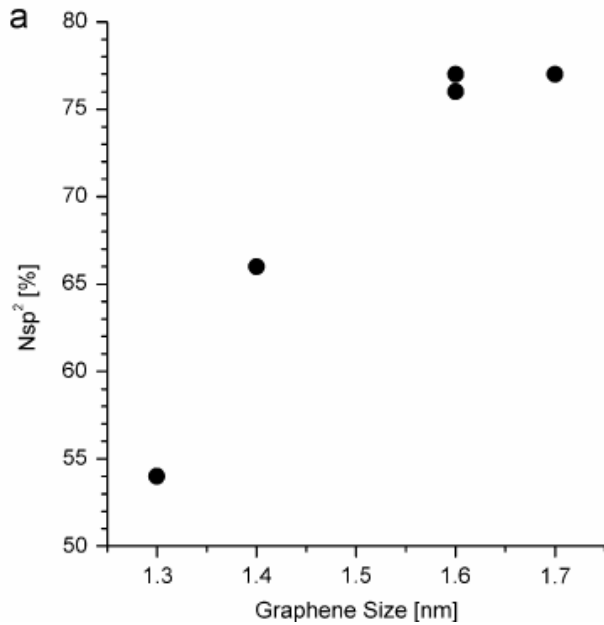
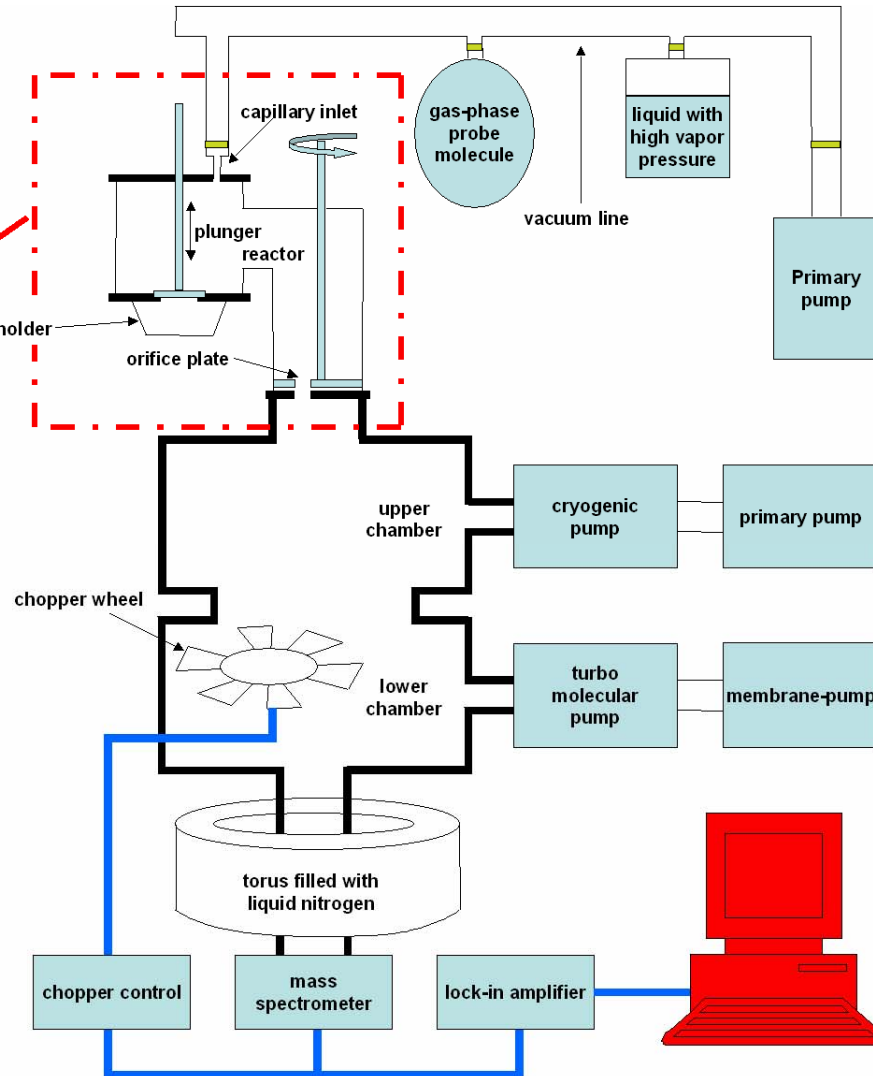


**Fig. 7** (a) Correlation of graphene size and Nsp<sup>2</sup> value. The larger the graphenes, the higher the sp<sup>2</sup> hybridization. (b) Correlation of the calculated curvature and Nsp<sup>2</sup> value. The strong bent graphenes exhibit a low sp<sup>2</sup> hybridization. (c) Correlation of graphene size and O<sub>2</sub> content. The larger the graphenes, the lower the O<sub>2</sub> content.

## Various Ways at Characterizing soot particles

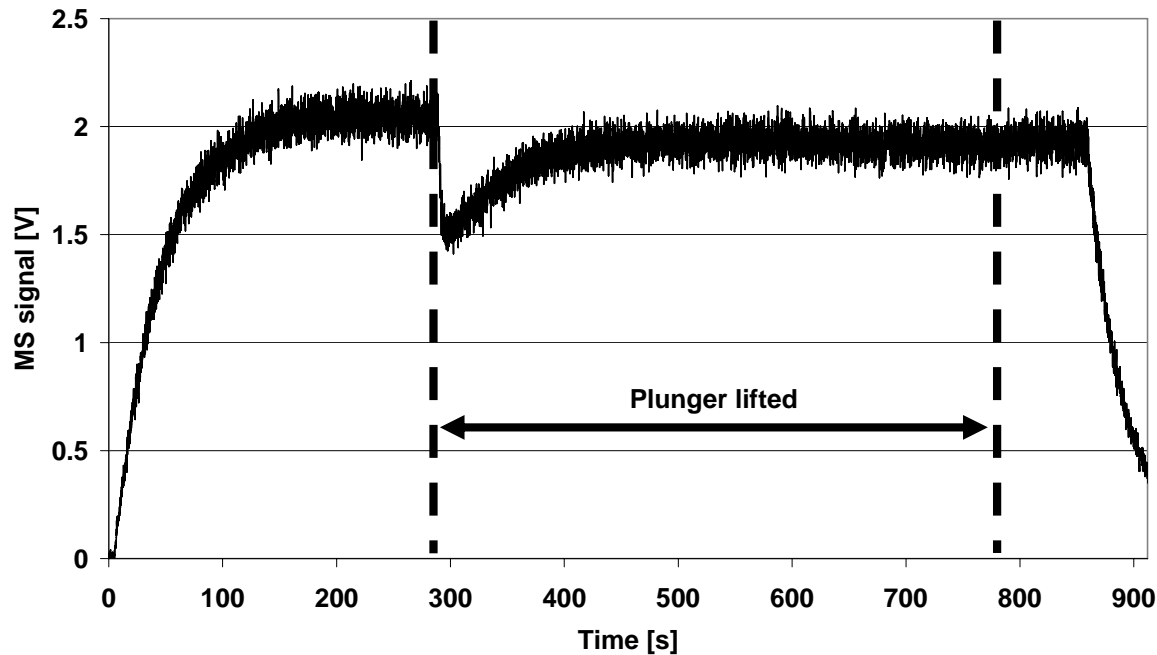
- Thermal Behavior: Pyrolysis, thermogravimetric measurement
- Extraction Behavior: Organic Phase vs. Elemental Carbon (OC/EC) or WSOC/WinSOC, etc.
- Elemental Analysis (C, H, N, O)
- Surface Spectroscopies (XRD, EELS, XPS)
- Imaging (ESEM, HRTEM)
- **Chemical** Composition of the Interface: this approach

# Knudsen Flow reactor



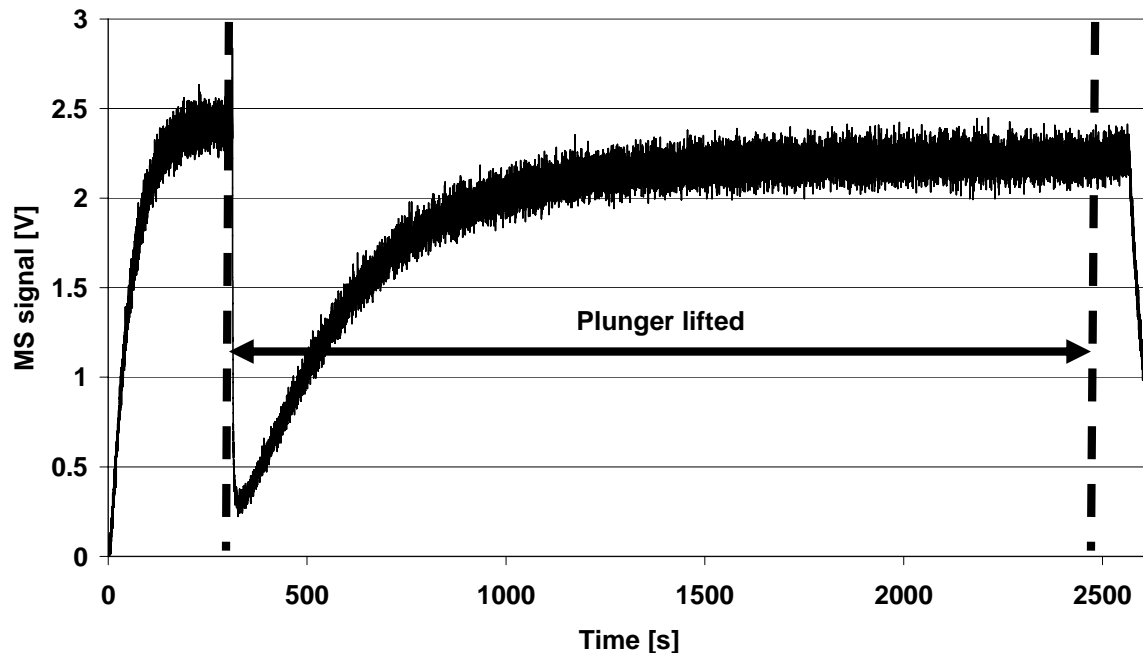


**N(CH<sub>3</sub>)<sub>3</sub> uptake on FS 101**



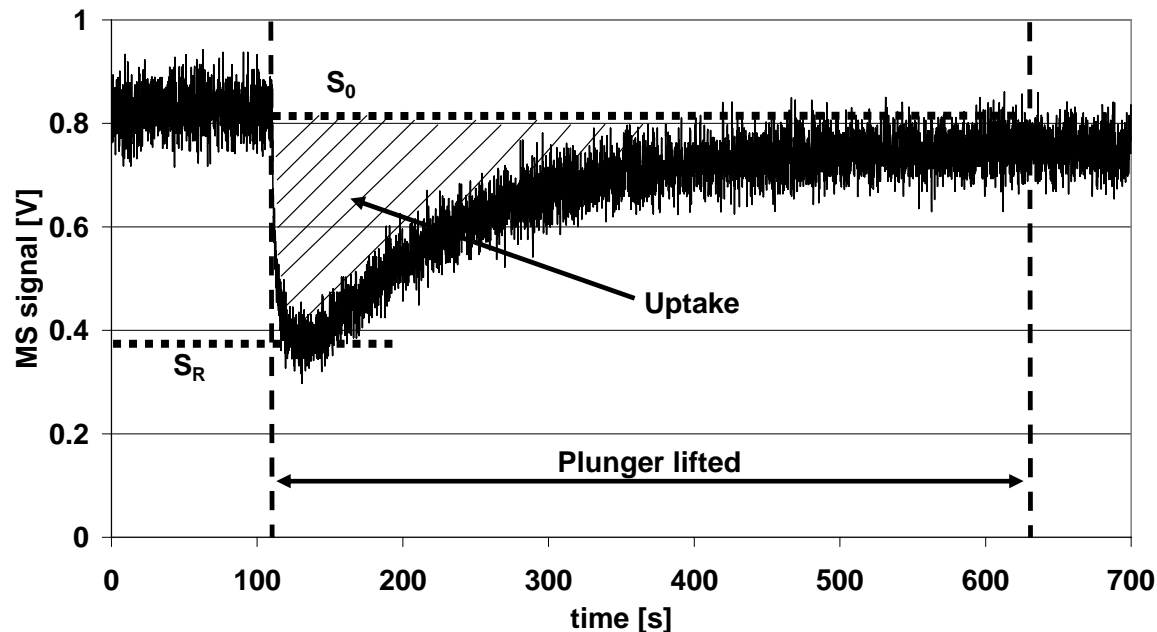
Raw data of N(CH<sub>3</sub>)<sub>3</sub> uptake on 10.0 mg amorphous carbon FS 101 at a flow rate of  $6.4 \times 10^{14}$  molecule s<sup>-1</sup> monitored at m/e 58 in the 1 mm diameter aperture Knudsen flow reactor ( $k_{\text{esc}} = 0.0308 \text{ s}^{-1}$ ) leading to the initial uptake coefficient  $\gamma_0 = 2.0 \times 10^{-4}$ .

**CF<sub>3</sub>COOH uptake on FW 2**



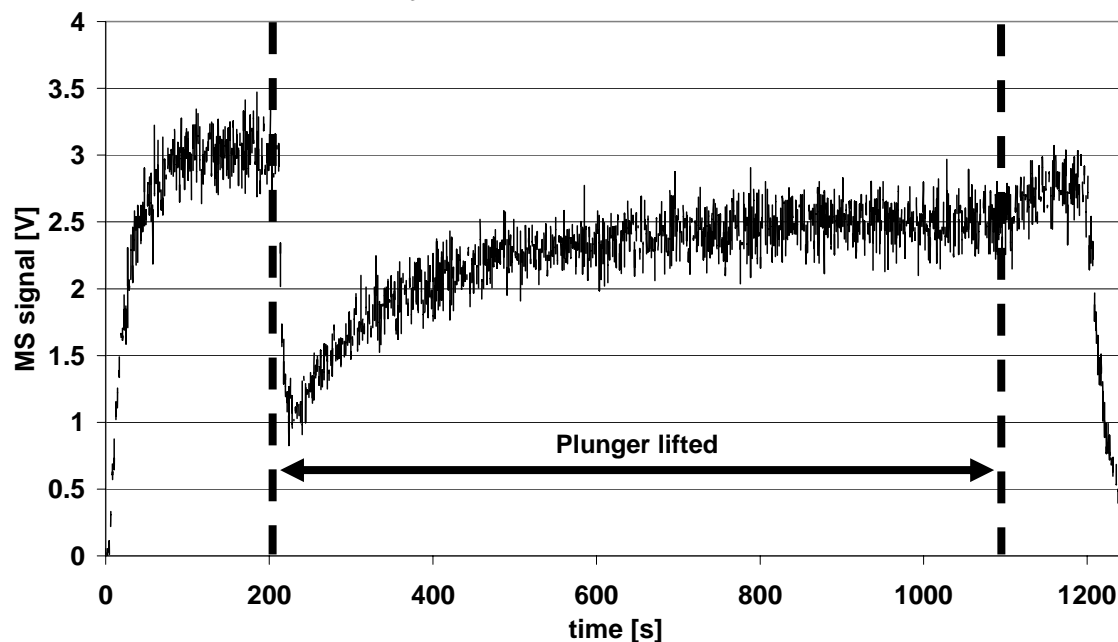
Raw data of CF<sub>3</sub>COOH uptake on 1.77 mg of amorphous carbon FW 2 at a flow rate of  $2.8 \times 10^{14}$  molecule s<sup>-1</sup> monitored at m/e 45 in the 1 mm diameter aperture Knudsen flow reactor ( $k_{\text{esc}} = 0.0214 \text{ s}^{-1}$ ) leading to the initial uptake coefficient  $\gamma_0 = 3.9 \times 10^{-3}$ .

### HCl uptake on aerosols collected in the field



Typical raw data of a titration experiment using the Knudsen flow reactor. Sample: aerosols collected in the bus depot 2 (23.05.2006, daytime) on silanized quartz fiber filter. Probe gas: HCl.  $m/z$ : 36.  $S_0$ : mass spectrometer signal at steady state.  $S_R$ : mass spectrometer signal immediately after the beginning of the reaction.

### O<sub>3</sub> vs hexane soot rich flame



Raw data of O<sub>3</sub> uptake on 1.14 mg of soot from a rich hexane flame at a flow rate of  $6.7 \times 10^{15}$  molecule s<sup>-1</sup> monitored at  $m/e$  48 in the 1 mm diameter aperture Knudsen flow reactor ( $k_{\text{esc}} = 0.0509$  s<sup>-1</sup>) leading to the initial uptake coefficient  $\gamma_0 = 1.6 \times 10^{-3}$ .

## Four Families of Probe Reactions

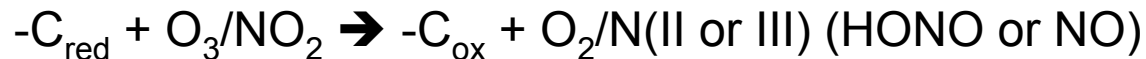
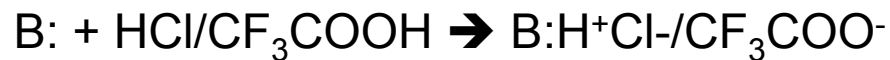
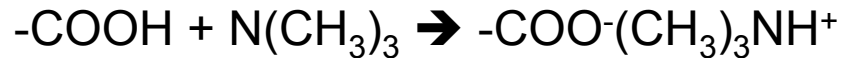
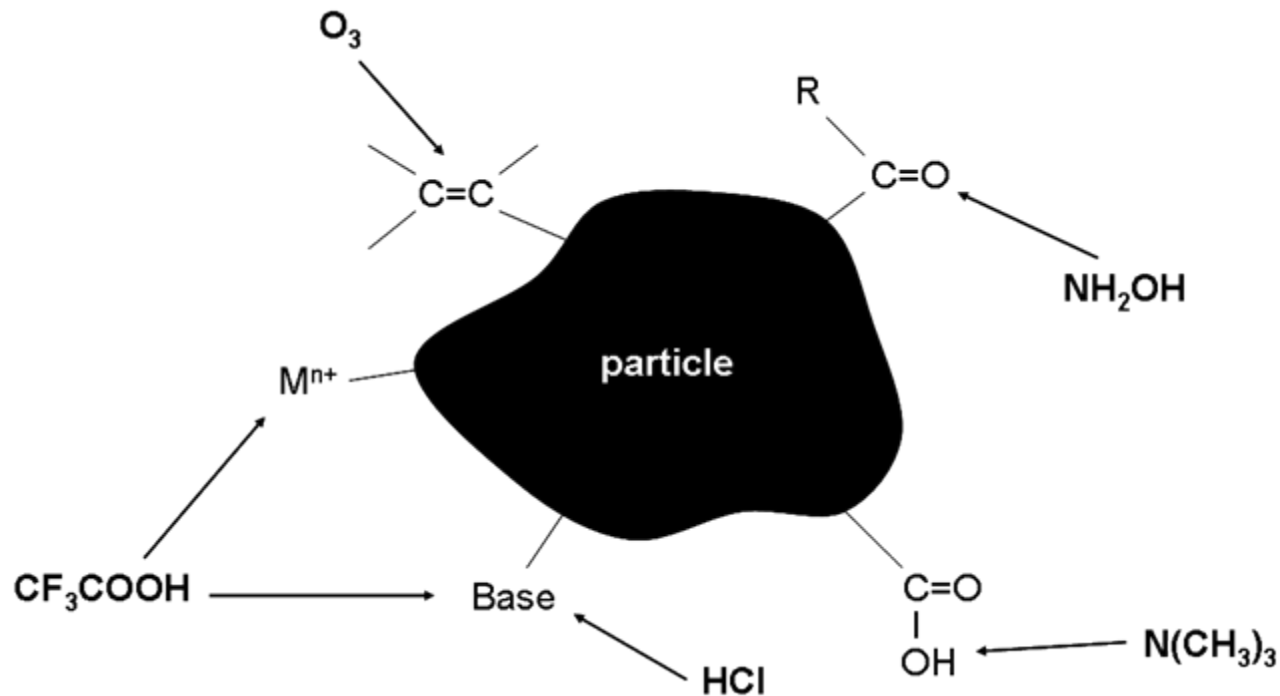


Table 1: Expected chemical reactions taking place with the different probes used in this work.

	Probes $\text{N}(\text{CH}_3)_3$	$\text{NH}_2\text{OH}$	$\text{CF}_3\text{COOH}$	$\text{HCl}$	$\text{O}_3$
Probe main characteristics	Base, weak ligand	Oxime formation with carbonyls	Very strong acid in the gas phase	Strong acid in the gas phase	Oxydant
Reacts with	Brönsted/Lewis acids -COOH -OH/Lactol -Metals (?) - $\text{NH}_4^+$	Electrophiles - C=O	Brönsted/Lewis bases -Amines -Metals -Pyrone structure	Brönsted/Lewis bases -Amines -Metals -Pyrone structure	-Unsaturation - Adsorbed $\text{NO}_x$ ( ?)

## Three **Constraints** for observing a titration reaction:

- Reactions must be fast (time scale of  $1/k_{\text{esc}} \sim 10$  s)
- Reactions are occurring at low pressure:  $\sim 10^{-3}$  mbar
- Reactions must occur at ambient temperature



$N_i^M/\text{mg}$  $N_i^M/\text{cm}^2$  $N_i^M/\text{ML}$ UPTAKES of Probe Gases ( $N_i^M$ )

	Surface BET [m <sup>2</sup> /g]	N(CH <sub>3</sub> ) <sub>3</sub>	NH <sub>2</sub> OH	CF <sub>3</sub> COOH	HCl	O <sub>3</sub>	NO <sub>2</sub>
FS 101	20 <sup>a</sup>	5.8 · 10 <sup>14</sup> 2.9 · 10 <sup>12</sup> 0.81	1.2 · 10 <sup>16</sup> 6.0 · 10 <sup>13</sup> 7.6	1.8 · 10 <sup>15</sup> 9.2 · 10 <sup>12</sup> 2.3	No reaction	7.3 · 10 <sup>17</sup> 3.7 · 10 <sup>15</sup> 498.0	2.0 · 10 <sup>15</sup> 9.8 · 10 <sup>12</sup> 1.4
Printex 60	115 <sup>a</sup>	1.5 · 10 <sup>15</sup> 1.3 · 10 <sup>12</sup> 0.36	2.1 · 10 <sup>16</sup> 1.8 · 10 <sup>13</sup> 2.3	4.0 · 10 <sup>15</sup> 3.5 · 10 <sup>12</sup> 0.9	8.2 · 10 <sup>14</sup> 7.1 · 10 <sup>11</sup> 0.08	6.4 · 10 <sup>16</sup> 5.6 · 10 <sup>13</sup> 7.5	7.4 · 10 <sup>15</sup> 6.4 · 10 <sup>12</sup> 0.90
FW 2	460 <sup>a</sup>	2.4 · 10 <sup>17</sup> 5.2 · 10 <sup>13</sup> 14.5	4.4 · 10 <sup>17</sup> 9.6 · 10 <sup>13</sup> 12.2	4.5 · 10 <sup>16</sup> 9.9 · 10 <sup>12</sup> 2.5	No reaction	4.4 · 10 <sup>17</sup> 9.6 · 10 <sup>13</sup> 12.9	4.1 · 10 <sup>16</sup> 8.9 · 10 <sup>12</sup> 1.3
SRM 2975	91	4.9 · 10 <sup>16</sup> 5.3 · 10 <sup>13</sup> 14.7	1.3 · 10 <sup>18</sup> 1.5 · 10 <sup>15</sup> 191.1	No reaction	2.4 · 10 <sup>15</sup> 2.6 · 10 <sup>12</sup> 0.3	8.3 · 10 <sup>15</sup> 9.1 · 10 <sup>12</sup> 1.2	3.2 · 10 <sup>15</sup> 3.5 · 10 <sup>12</sup> 0.49
Diesel TPG	53.2	3.1 · 10 <sup>16</sup> 5.8 · 10 <sup>13</sup> 16.1	1.4 · 10 <sup>18</sup> 2.6 · 10 <sup>15</sup> 331.2	No reaction	4.6 · 10 <sup>16</sup> 8.7 · 10 <sup>13</sup> 10.1	1.3 · 10 <sup>17</sup> 2.5 · 10 <sup>14</sup> 33.7	1.3 · 10 <sup>16</sup> 2.4 · 10 <sup>13</sup> 3.4
Hexane soot from rich flame	48.9	1.8 · 10 <sup>15</sup> 3.8 · 10 <sup>12</sup> 1.1	2.1 · 10 <sup>17</sup> 4.4 · 10 <sup>14</sup> 55.7	1.8 · 10 <sup>15</sup> 3.8 · 10 <sup>12</sup> 0.9	9.0 · 10 <sup>15</sup> 1.9 · 10 <sup>13</sup> 2.2	9.5 · 10 <sup>17</sup> 2.0 · 10 <sup>15</sup> 266.4	2.6 · 10 <sup>16</sup> 5.4 · 10 <sup>13</sup> 7.6
Hexane soot from lean flame	74.3	2.8 · 10 <sup>15</sup> 3.8 · 10 <sup>12</sup> 1.1	3.3 · 10 <sup>17</sup> 4.5 · 10 <sup>14</sup> 56.8	3.2 · 10 <sup>15</sup> 4.3 · 10 <sup>12</sup> 1.1	3.1 · 10 <sup>15</sup> 4.2 · 10 <sup>12</sup> 0.5	2.0 · 10 <sup>18</sup> 2.7 · 10 <sup>15</sup> 364.0	1.9 · 10 <sup>16</sup> 2.6 · 10 <sup>13</sup> 3.6

## RESULTS on UPTAKES $N_i^M$ on Carbonaceous Nanoparticles

▶ FW2, SRM, Diesel TPG: High Acidity, highly oxidized –  $N(CH_3)_3$  probe

▶ SRM, Diesel TPG, hexane flames: Carbonyl (ketones, aldehydes), partial oxidation –  $NH_2OH$  probe

▶ Except for SRM, Diesel TPG: basic and acid sites are roughly balanced

▶ Am. Carbons, lean hexane soot, Ratio  $N_i^{CF_3COOH}/NiHCl > 1$ : suggests presence of basic oxides (react with acids)

▶ FS101, hexane soot: oxidizable surface –  $O_3$  probe. Other extreme: SRM (per-oxidized).

▶ Diesel TPG, hexane soot (lean, rich): easily oxidizable –  $NO_2$  probe

# Uptakes ( $N_i^M$ ) for Limonene and Toluene SOA, Toluene Soot

Demirdjian, 2005 (Atmos. Chem. Phys. Discuss.)

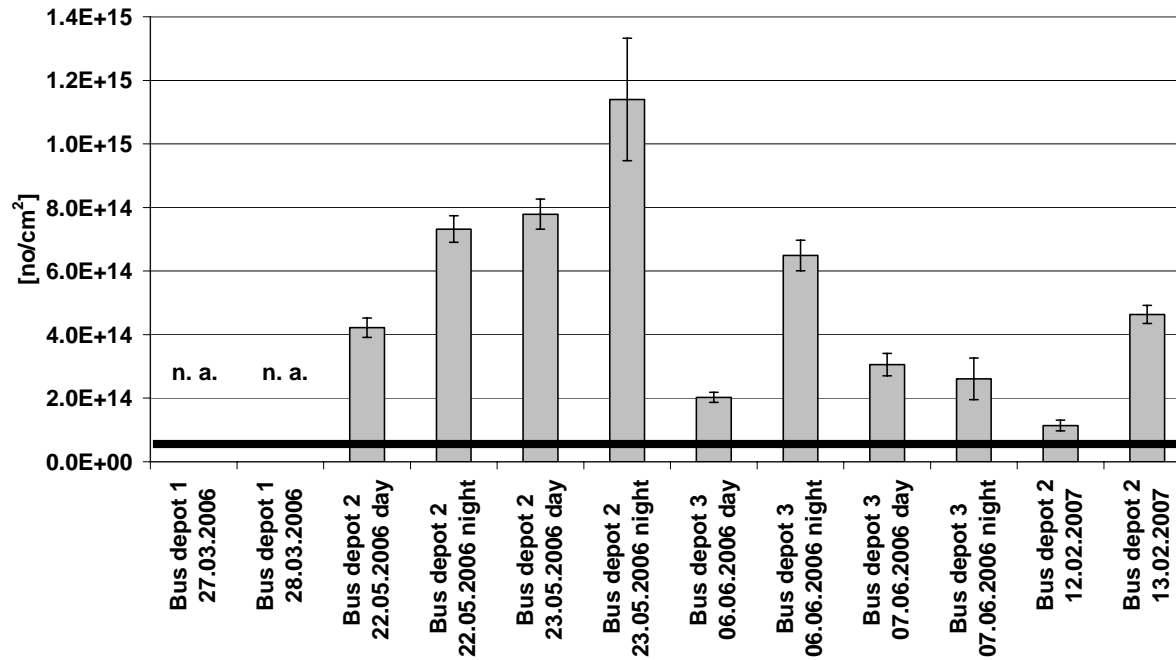
	$O_3$		$NO_2$		$(CH_3)_3N$		$NH_2OH$	
	$N_{O_3}/M_{SOA}^d$ $N_{O_3}/S^e$ ML(%) <sup>f</sup>	product	$N_{NO_2}/M_{SOA}^d$ $N_{NO_2}/S^e$ ML(%) <sup>f</sup>	product	$N_{NMe_3}/M_{SOA}^d$ $N_{NMe_3}/S^e$ ML(%) <sup>f</sup>	product	$N_{NH_2OH}/M_{SOA}^d$ $N_{NH_2OH}/S^e$ ML(%) <sup>f</sup>	product
limonene SOA <sup>a</sup>	no reactivity		no reactivity		$(2.1 \pm 0.1) \times 10^{15}$ $(1.2 \pm 0.1) \times 10^{13}$ 5.0	(salt)	$(1.3 \pm 0.1) \times 10^{18}$ $(7.6 \pm 0.1) \times 10^{15}$ > $\times 31.7^g$ Lower Limit	(oxime)
toluene SOA <sup>b</sup>	no reactivity	-	no reactivity	-	$(1.3 \pm 0.2) \times 10^{15}$ $(1.1 \pm 0.2) \times 10^{13}$ 3.4	(salt)	$(9.3 \pm 0.3) \times 10^{15}$ $(7.6 \pm 0.2) \times 10^{13}$ 23.7	(oxime)
toluene soot <sup>c</sup>	$(2.0 \pm 0.2) \times 10^{17}$ $(2.0 \pm 0.2) \times 10^{14}$ 100.0	$O_2$	$(1.8 \pm 0.2) \times 10^{16}$ $(1.8 \pm 0.2) \times 10^{13}$ 9.0	HONO	$(4.0 \pm 0.2) \times 10^{15}$ $(4.0 \pm 0.2) \times 10^{12}$ 2.0	(salt)	no reactivity	-

<sup>a</sup>  $N_{lim} = 2.4 \times 10^{14}$  molecule  $cm^{-2}$  per monolayer (ML).

<sup>b</sup>  $N_{tol} = 3.2 \times 10^{14}$  molecule  $cm^{-2}$  per ML.

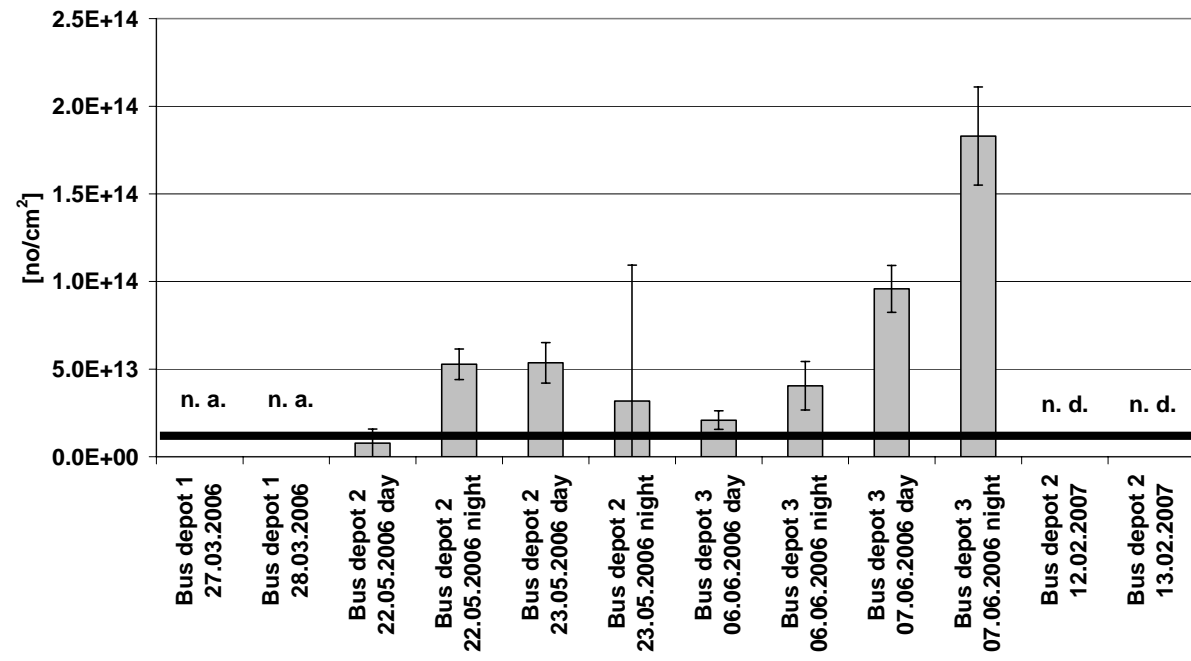
<sup>c</sup>  $N_C = 2.0 \times 10^{14}$  molecule  $cm^{-2}$  per ML.

### HCl



Field Measurement: aerosol sampling in bus depot

### N(CH<sub>3</sub>)<sub>3</sub>





# Uptake probabilities ( $\gamma_0$ ) rel. to geometric surface

	$\text{N}(\text{CH}_3)_3$	$\text{NH}_2\text{OH}$	$\text{CF}_3\text{COOH}$	$\text{HCl}$	$\text{O}_3$	$\text{NO}_2$
<b>FS 101</b>	$7.8 (\pm 0.4) \cdot 10^{-4}$	$6.1 (\pm 1.0) \cdot 10^{-4}$	$7.9 (\pm 0.6) \cdot 10^{-3}$	no reaction	$1.1 (\pm 0.1) \cdot 10^{-2}$	$3.8 (\pm 0.3) \cdot 10^{-4}$
<b>Printex 60</b>	$9.9 (\pm 0.6) \cdot 10^{-4}$	$9.9 (\pm 1.7) \cdot 10^{-4}$	$2.2 (\pm 0.2) \cdot 10^{-2}$	$2.1 (\pm 0.1) \cdot 10^{-3}$	$1.0 (\pm 0.1) \cdot 10^{-1}$	$1.8 (\pm 0.2) \cdot 10^{-3}$
<b>FW 2</b>	$4.3 (\pm 0.2) \cdot 10^{-2}$	$4.4 (\pm 0.7) \cdot 10^{-2}$	$1.6 (\pm 0.1) \cdot 10^{-2}$	no reaction	$1.1 (\pm 0.1) \cdot 10^{-1}$	$5.8 (\pm 0.5) \cdot 10^{-3}$
<b>SRM 2975</b>	$2.4 (\pm 0.1) \cdot 10^{-2}$	$1.5 (\pm 0.3) \cdot 10^{-2}$	no reaction	$2.9 (\pm 0.1) \cdot 10^{-3}$	$5.8 (\pm 0.5) \cdot 10^{-4}$	$6.3 (\pm 0.5) \cdot 10^{-4}$
<b>Diesel TPG</b>	$1.3 (\pm 0.1) \cdot 10^{-2}$	$2.1 (\pm 0.4) \cdot 10^{-2}$	no reaction	$1.3 (\pm 0.1) \cdot 10^{-2}$	$1.0 (\pm 0.1) \cdot 10^{-2}$	$1.4 (\pm 0.1) \cdot 10^{-3}$
<b>Hexane lean flame</b>	$8.7 (\pm 0.5) \cdot 10^{-5}$	$1.5 (\pm 0.3) \cdot 10^{-3}$	$2.9 (\pm 0.2) \cdot 10^{-3}$	$1.7 (\pm 0.1) \cdot 10^{-4}$	$2.4 (\pm 0.2) \cdot 10^{-2}$	$2.5 (\pm 0.2) \cdot 10^{-3}$
<b>Hexane rich flame</b>	$8.4 (\pm 0.5) \cdot 10^{-5}$	$4.2 (\pm 0.7) \cdot 10^{-4}$	$3.6 (\pm 0.3) \cdot 10^{-4}$	$2.0 (\pm 0.1) \cdot 10^{-4}$	$1.6 (\pm 0.1) \cdot 10^{-3}$	$2.8 (\pm 0.2) \cdot 10^{-3}$

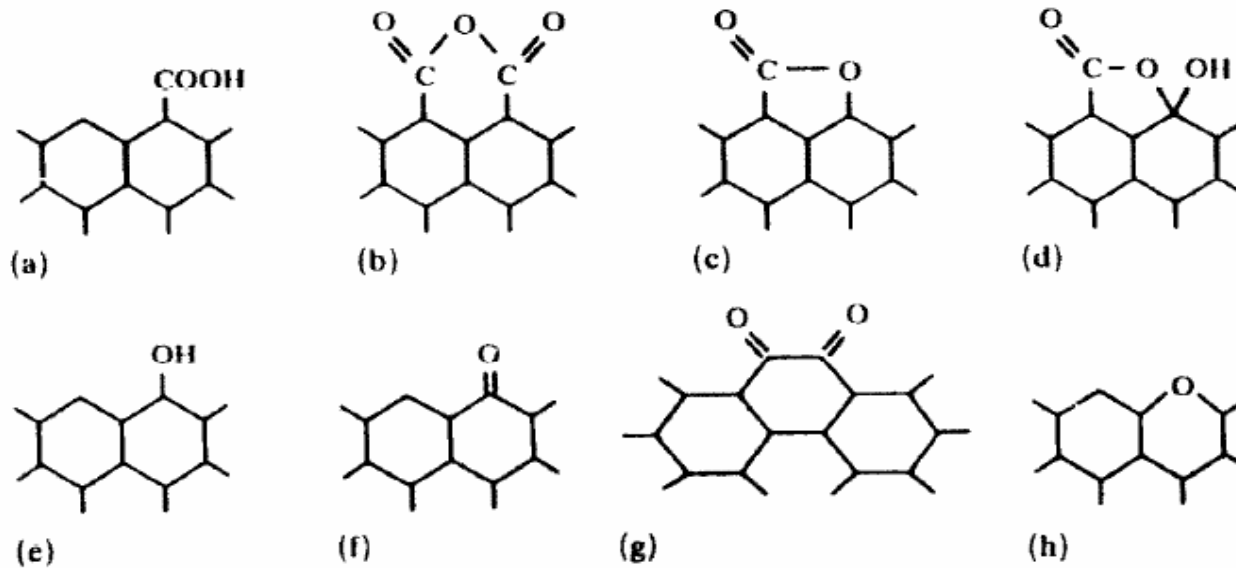


Fig. 1. Possible structures of surface oxygen groups (see text).

## ACIDIC SITES

## BASIC SITES

U. Hofmann et al; H.P. Boehm et al.

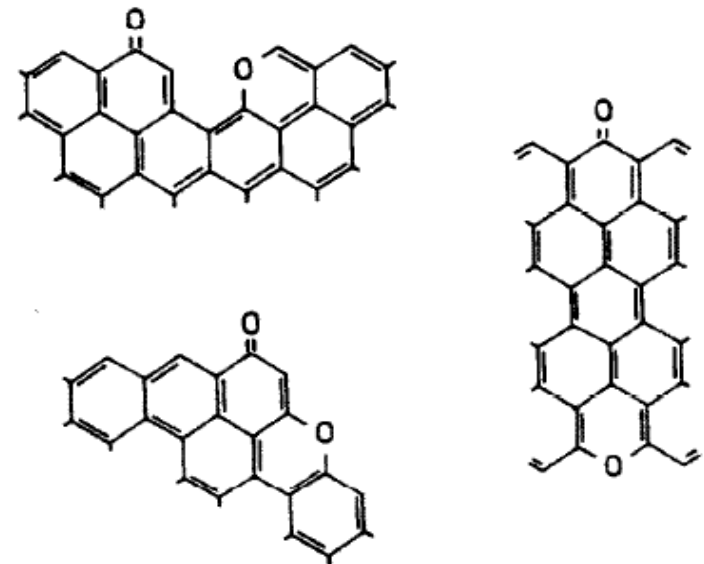
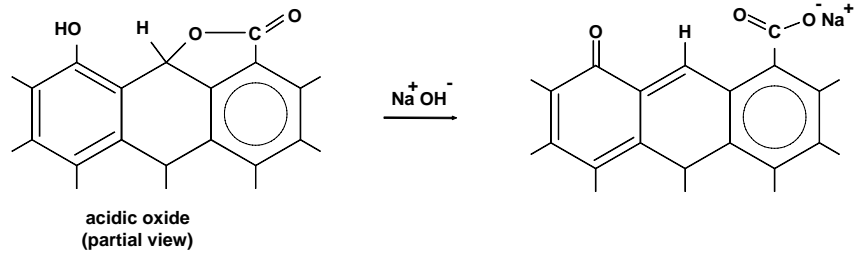
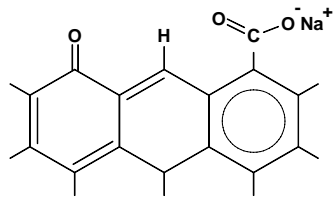


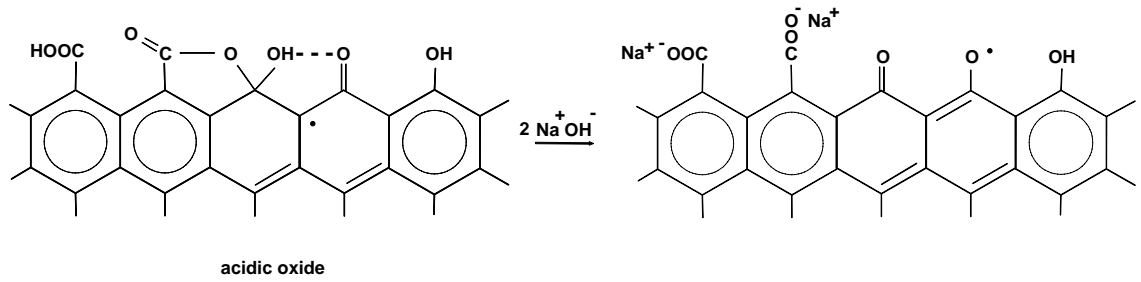
Fig. 5. Possible structures of basic surface sites on a graphene layer, derived from the  $\gamma$ -pyrone structure.



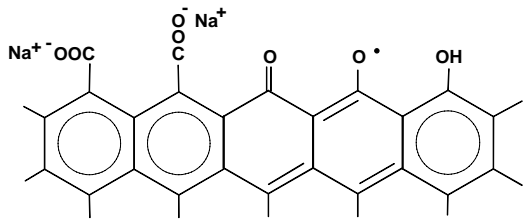
A



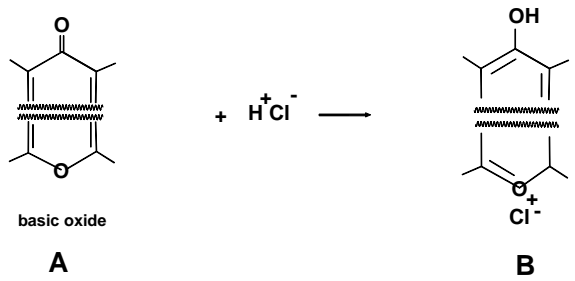
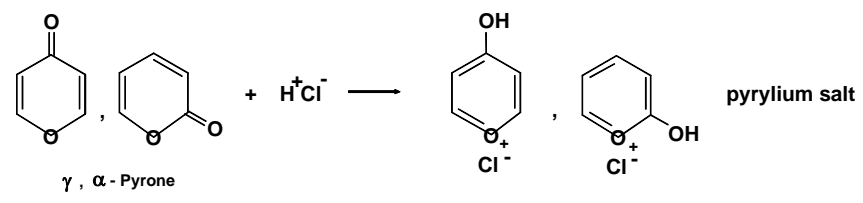
B



C



D



A

B

## CONCLUSIONS

- Combustion Source determines surface/interface composition
- Surface is multifunctional, e.g. acidic and basic surface sites coexist
- Method allows QUANTITATIVE comparison between aerosols of different origin, e.g. combustion vs. Environmental in terms of  $N_i^M$  and  $\gamma_0$
- Environmental aerosol are more reactive w/r to certain categories than « fresh » combustion particles. AGING?

<b>Setyan A.</b>	<i>Assessment of Diesel Exhaust Particulate Exposure and Surface Characteristics in Association with Levels of Oxidative Stress Biomarkers</i>
------------------	--

### Forthcoming Papers:

**Characterization of surface functional groups present on ambient ultrafine and fine particles by heterogeneous titration reactions**

*Ari Setyan<sup>a</sup>, Jean-Jacques Sauvain<sup>a</sup>, Michael Riediker<sup>a</sup>, Michel Guillemin<sup>a</sup>, Michel J. Rossi<sup>b</sup>*

<sup>a</sup> Institute for Work and Health, University of Lausanne and University of Geneva, Rue du Bugnon 21, CH-1005 Lausanne, Switzerland

<sup>b</sup> Swiss Federal Institute of Technology, Air and Soil Pollution Laboratory, Station 6, CH-1015 Lausanne, Switzerland

**Characterization of Functional Groups at the Gas – Particle Interface of amorphous carbon, Diesel, hexane flame soot and TiO<sub>2</sub> Nanoparticles using Heterogeneous Chemistry**

*A. Setyan<sup>a</sup>, J.-J. Sauvain<sup>a</sup> and M.J. Rossi<sup>b\*</sup>*

<sup>a</sup> Institut Universitaire Romand de Santé au Travail (IST), Université de Lausanne et Université de Genève, rue du Bugnon 21, CH-1005 Lausanne

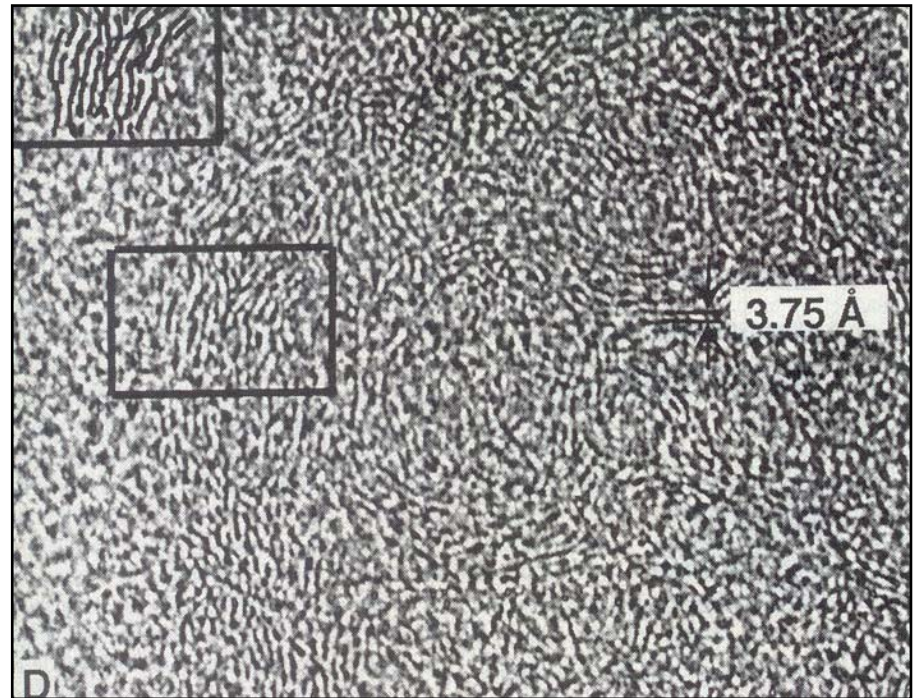
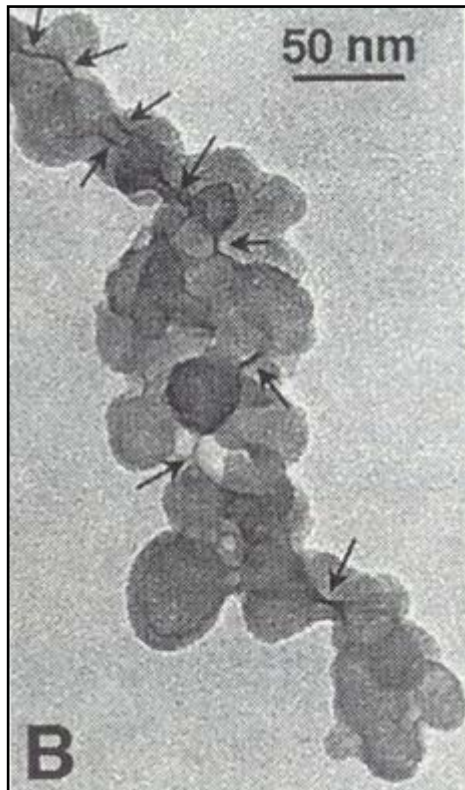
<sup>b</sup> Laboratoire de Pollution Atmosphérique et Sol (LPAS), Ecole Polytechnique Fédérale de Lausanne (EPFL), Station 6, CH-1015 Lausanne



ÉCOLE POLYTECHNIQUE  
FÉDÉRALE DE LAUSANNE

## Soot Structural Aspects

Particles in the marine boundary layer are internal mixtures of ammonium sulfate ( $(\text{NH}_4)_2\text{SO}_4$ ) and soot (Posfai, 1999). Right graph shows the disordered graphitic layers of soot particles.



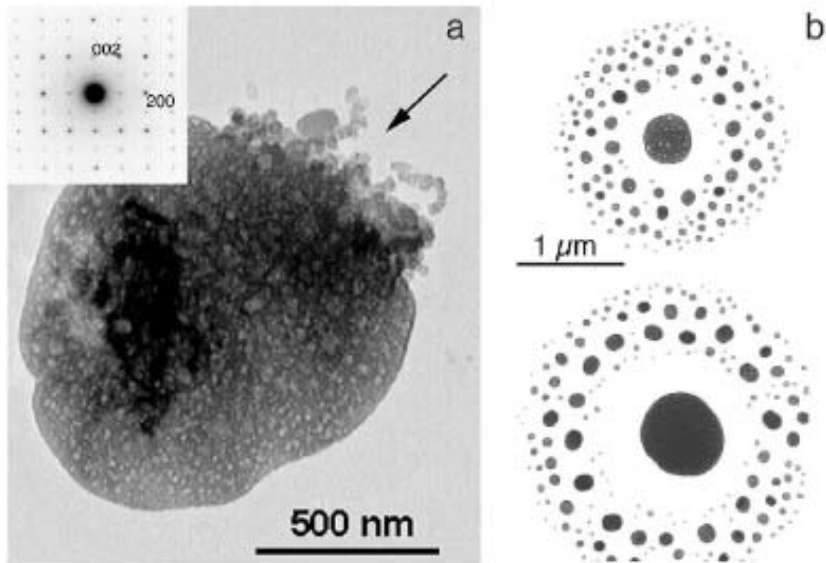


FIG. 1. TEM images of  $(\text{NH}_4)_2\text{SO}_4$ . (a) The selected-area electron-diffraction pattern (upper left) confirms the identification. The arrow points to a soot aggregate. (Azores, North Atlantic, ASTEX/MAGE); (b) Rings of small  $(\text{NH}_4)_2\text{SO}_4$  crystals that formed as the sulfate particles dehydrated. The dimensions of the halos can be used to distinguish among particles that likely had different water contents while still airborne. (Southern Ocean, ACE-1.)

Buseck and Posfai, PNAS 1999

Aged Aerosol far from the source is a composite: soot,  $(\text{NH}_4)_2\text{SO}_4$ , gypsum, NaCl, etc.

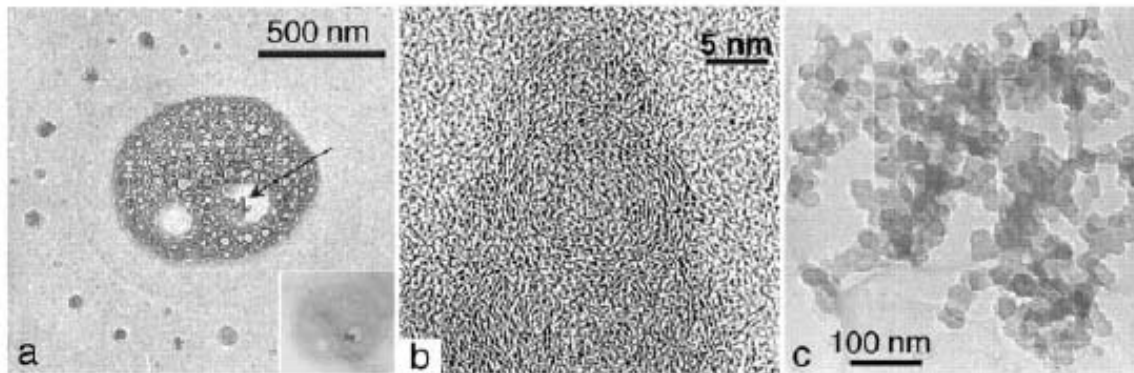


FIG. 2. TEM images of an internal mixture of  $(\text{NH}_4)_2\text{SO}_4$  and soot. (a) The halo is similar to those in Fig. 1. The arrow points to a soot aggregate. (Southern Ocean, ACE-1); (b) High-resolution image of the arrowed tip of the soot aggregate in a. A degree of ordering is evident in the onion-like graphitic layers, seen edge on. (c) A large branching soot aggregate; such aggregates are typical of combustion processes (95). (Southern Ocean, ACE-1.)



## Uptake Probabilities ( $\gamma_0$ ) rel. to BET surface

	$\text{N}(\text{CH}_3)_3$	$\text{NH}_2\text{OH}$	$\text{CF}_3\text{COOH}$	$\text{HCl}$	$\text{O}_3$	$\text{NO}_2$
<b>FS 101</b>	$3.9 (\pm 0.2) \cdot 10^{-7}$	$6.7 (\pm 1.1) \cdot 10^{-7}$	$2.4 (\pm 0.2) \cdot 10^{-6}$	no reaction	$1.6 (\pm 0.1) \cdot 10^{-5}$	$5.0 (\pm 0.4) \cdot 10^{-7}$
<b>Printex 60</b>	$1.5 (\pm 0.1) \cdot 10^{-7}$	$2.7 (\pm 0.5) \cdot 10^{-7}$	$1.1 (\pm 0.1) \cdot 10^{-6}$	$6.8 (\pm 0.3) \cdot 10^{-7}$	$1.7 (\pm 0.1) \cdot 10^{-5}$	$4.9 (\pm 0.4) \cdot 10^{-7}$
<b>FW 2</b>	$8.8 (\pm 0.5) \cdot 10^{-6}$	$2.5 (\pm 0.4) \cdot 10^{-6}$	$1.9 (\pm 0.2) \cdot 10^{-6}$	no reaction	$1.2 (\pm 0.1) \cdot 10^{-5}$	$5.7 (\pm 0.5) \cdot 10^{-7}$
<b>SRM 2975</b>	$1.3 (\pm 0.1) \cdot 10^{-5}$	$1.4 (\pm 0.2) \cdot 10^{-5}$	no reaction	$1.5 (\pm 0.1) \cdot 10^{-6}$	$2.4 (\pm 0.2) \cdot 10^{-7}$	$3.0 (\pm 0.3) \cdot 10^{-7}$
<b>Diesel STA</b>	$1.2 (\pm 0.1) \cdot 10^{-5}$	$1.6 (\pm 0.3) \cdot 10^{-5}$	no reaction	$1.2 (\pm 0.1) \cdot 10^{-5}$	$6.6 (\pm 0.6) \cdot 10^{-6}$	$1.3 (\pm 0.1) \cdot 10^{-6}$
<b>Hexane rich flame</b>	$3.6 (\pm 0.2) \cdot 10^{-8}$	$3.4 (\pm 0.6) \cdot 10^{-7}$	$7.8 (\pm 0.6) \cdot 10^{-8}$	$1.3 (\pm 0.1) \cdot 10^{-7}$	$2.8 (\pm 0.2) \cdot 10^{-6}$	$1.1 (\pm 0.1) \cdot 10^{-6}$
<b>Hexane lean flame</b>	$3.2 (\pm 0.2) \cdot 10^{-8}$	$5.1 (\pm 0.9) \cdot 10^{-7}$	$6.2 (\pm 0.5) \cdot 10^{-7}$	$3.3 (\pm 0.1) \cdot 10^{-8}$	$8.7 (\pm 0.7) \cdot 10^{-6}$	$6.2 (\pm 0.5) \cdot 10^{-7}$